Innate Immune Response Against COVID-19: The First Report on the Theory of COVID-19 Treatment by a Combined Method of Mathematics and Medicine

M. Lotfi
University of Tabriz
A. Jabbari (a_jabari@tabrizu.ac.ir)
University of Tabriz
R. Rahbarghazi
Tabriz University of Medical Sciences
H. Kheiri
University of Tabriz

Research Article

Keywords: COVID-19, SARS-CoV-2, Innate immune response, In-host model, Mathematical modeling

Posted Date: August 24th, 2021

DOI: https://doi.org/10.21203/rs.3.rs-806172/v1

Innate immune response against COVID-19: The first report on the theory of COVID-19 treatment by a combined method of mathematics and medicine

M. Lotfi[a], A. Jabbari[b*], R. Rahbarghazi[c], H. Kheiri[a]

[a] *Department of Applied Mathematics, Faculty of Mathematical Sciences, University of Tabriz, Tabriz, Iran*

[b] *Marand Faculty of Engineering, University of Tabriz, Tabriz, Iran*

[c] *Department of Applied Cell Sciences, Faculty of Advanced Medical Sciences, Tabriz University of Medical Sciences, Tabriz, Iran*

[*] *Corresponding author: A. Jabbari, a_jabari@tabrizu.ac.ir*

Abstract

Coronavirus disease 19 (COVID-19) continues to challenge most scientists searching for an effective way to diminish global outbreaks. As a correlate, progress in our knowledge about the COVID-19 has occurred, and we are more acknowledged than the early stages of a pandemic. However, these efforts have not been enough to stop the viral transmission, and many questions remain unanswered. To this end, understanding the interaction between SARS-CoV-2 and target cells affected by this virus is mandatory. Along with studies in the field of the clinical setting and basic research, some achievements in the modeling and analysis of COVID-19 disease have been obtained in mathematics. Unfortunately, these models are not comprehensive to predict or approve of which occur inside the body after virus entry. Commensurate with these comments, models with more elaborate structures and minimum failure rate prediction are highly demanded. Here, we aimed to systematically construct the modeling of the interaction between the SARS-CoV-2 virus and innate immune system cells and especially analyze the invasion of the virus to epithelial cells.

Keywords: COVID-19, SARS-CoV-2, Innate immune response, In-host model, Mathematical modeling.

Introduction

Infectious disease epidemics are one of the most severe challenging threats that humankind historically has faced. From the past to the present, humans have been confronted with infectious diseases such as the Plague of Justinian, the first known pandemic on record [1], and the Black Death occurred in 541-542 AD and fourteenth century, respectively. Smallpox is another devastating disease that has killed more people than all the wars in history. Cholera was, of course, a considerable concern in the nineteenth century and remains a concern today, especially in places like Bangladesh[2]. All of these and other kinds of infectious diseases are the best examples that reveal the importance of how an epidemic disease can challenge human life. At the end of 2019, the world has experienced a novel coronavirus (SARS-CoV-2 virus) infection with the complication of the pulmonary tract (respiratory system) was reported in Wuhan, (Hubei province, China). While China put great effort into preventing the spread of this virus, COVID-19 has, unfortunately, developed to more than 210 countries moving from the epidemic center to remote places, leading to the global pandemic. Based on the clinical investigations, SARS-CoV-2 has been so far (13 July 2021) responsible for more than 186 million cases of infection and more than 4 million deaths worldwide [3]. The primary target of SARS-CoV-2 infection is the lower respiratory tract causing Flu-like illness with symptoms such as cough, fever, fatigue, and arthralgia[4]. Studies targeting this pandemic have reached some helpful information in the treatment and vaccine development. Despite these advances, COVID-19 still kills the population, and efforts are still ongoing to find appropriate medication or approaches to prohibit COVID-19 infection and, or decrease the horizontal transmission of the SARS-CoV-2 virus in societies. Historically, coronaviruses are members of the family Coronaviridae (viral particles contain single-stranded RNA) can infect different species such as bats, camels, cats, and dogs, etc. The horizontal transmission of viral particles happens by airborne droplets after coughing or sneezing. Although many mathematical models in epidemiology have been developed to address whether and how individual behavior

(e.g., early self-isolation, wear masking, and social distancing) and preventive strategies such as hand washing and covering coughs and sneezes can control the spread of COVID-19 [5, 6, 7, 8, 9, 10, 11], there are too few models at an in-host level to give us information about viral replication in the target cell (s), the reciprocal interaction between the virus and immune response system and effect of medications and therapeutic agents on the induction of immune cell response against SARS-CoV-2 virus in vivo condition. Even though, previous in-host mathematical models are too elementary[12, 13, 14]. Here, it is worth mentioning that mathematical modeling at the level of epidemiological remarkably assists politicians in passing effective laws in public health. Besides, within-host mathematical modeling helps medical scientists like virologists, immunologists, and pharmacists to understand better how COVID-19 disease starts and expand inside the human body at micro-levels. This research hopes to fill the knowledge gap on the interaction between human innate immune response and SARS-COV-2 virus, and be beneficial for mathematical biologists and biomedical researchers (virologists, immunologists, pharmacologists, etc.). The onset and performance of innate immune system response after SARS-COV-2 virus were predicted using mathematical modeling. Here, we briefly introduced the innate immune system to the understanding of the modeling section. The function of innate immune cells against the SARS-COV-2 was modeled step by step accurately using ordinary differential equations. Then, the constructed model was analyzed from the viewpoint of some mathematical aspects like both local and global stability. It is postulated that the result of this modeling can help pharmacologists in the development and production of effective vaccines and suitable antiviral therapies. In the next step, the proposed model was represented graphically to confirm the theoretical results. In the latter phase, modeling results were interpreted in terms of biological and medical aspects.

Innate immune response

Here, we present some fundamental functions of innate immune response cells because of better seeing immunity against the SARS-CoV-2 virus. Innate immunity is the first line of defense against internal and external pathogens. Upon the entrance or activation of pathogens, the innate immune response is initiated to reduce the possibility of infectious agent biodistribution. Innate immune responses are non-specific and occurred immediately (between

0-96 hours) after pathogens transmission. This system comprises various cell types from different lineages such as macrophages, mast cells, natural killer cells (NK cells), neutrophils, basophils, eosinophils, and dendritic cells. After production in bone marrow, these cells enter the systemic circulation.They are transferred into the peripheral tissues such as skin, mucous and epithelial layers, and connective tissues, where they can directly deal with the potential problems. As above-mentioned, neutrophils, basophils, eosinophils are members of granulocytes and function in the innate immune system. These cells contain numerous intracellular granules and release their contents after activation. In addition, they can engulf (phagocyte) the foreign bodies or other invasive agents. Both enzymatic reaction and phagocytosis can decoy the pathogen and prohibit further spreading inside the body. Macrophages, NK cells, and dendritic cells are other cellular components of innate responses. These cells can phagocyte the pathogens or secret different inflammatory biomolecules that regulate the innate response activity of neutrophils, basophils, and eosinophils. Of note, the member of the innate immune system works and communicates with adaptive (acquired) immune system cells in a regulated manner[15].

Model construction

Here, we aimed to develop a model in the dynamic of an in-host mathematical model of COVID-19. To be more specific, we collected data regarding the effect of the innate immune response against the SARS-COV-2 virus. In our developed model, as shown in figure 1, different state variables were considered. From a biological point of view, the state variables are immune cellular constitutes in which most are affected by the virus as follows: Suppose S_E represents the density of healthy epithelial cells, I_E, the density of infected epithelial cells. Also, let M_1 density of resting macrophages, M_2 density of activated macrophages. Assume C_N and C_M be the concentration of neutrophils and monocytes, respectively. Finally, let V be the number of virus particles. Therefore, the model for the within-host dynamic of the innate immune response against the SARS-COV2 virus was proposed by the

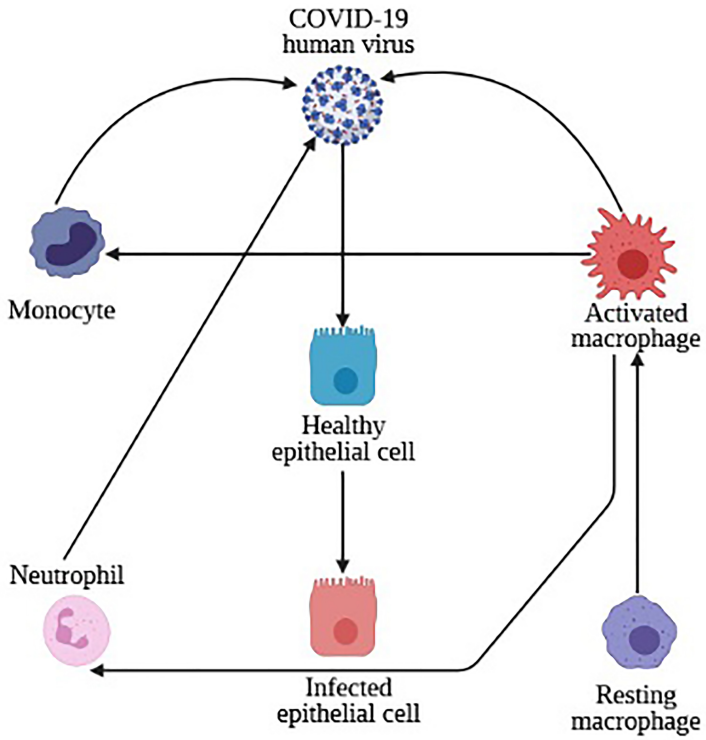

Figure 1: Main immune cellular constitutes of an innate immune response against SARS-COV-2 virus. Within minutes-hours of exposure to infectious agents, main immune cellular constitutes such as resting macrophages are frustrated and polarized to the activated form (activated macrophages). These cells can release numerous factors (biomolecules) that promote the recruitment of their progenies (monocytes) from the blood into the target organs, leading to increased macrophage density at the site of viral infection. Besides, activated macrophages produce arrays of inflammatory factors that trigger the function of granulocytes, such as neutrophils. The communication between different cellular constitutes of innate immune response can limit further replication (proliferation) and propagation of viral particles (SARS-COV-2 virus).

below non-linear system of differential equations

$$\begin{aligned}
\frac{dS_E}{dt} &= \psi_s - \xi S_E V - \mu_s S_E + \rho I_E, \\
\frac{dI_E}{dt} &= \xi S_E V - \mu_i I_E - \rho I_E, \\
\frac{dM_1}{dt} &= \psi_r - \alpha_r M_1 V - \mu_r M_1 + \kappa M_2, \\
\frac{dM_2}{dt} &= \alpha_r M_1 V - \mu_a M_2 - \kappa M_2 - \nu_a M_2 V, \\
\frac{dC_N}{dt} &= \psi_n M_2 C_N - \mu_n C_N - \nu_n C_N V, \\
\frac{dC_M}{dt} &= \psi_m M_2 C_M - \mu_m C_M - \nu_m C_M V, \\
\frac{dV}{dt} &= \eta \psi_v I_E - \mu_v V - \gamma_c M_2 V - \gamma_n C_N V - \gamma_m C_M V.
\end{aligned} \tag{1}$$

The associated parameters and variables are shown in the table 1.

Biological interperation of proposed model

(1) HECs constitute a single cell layer and cover the luminal surface of the mucosal layer and alveolar sacs. In normal conditions, these cells are repopulated after activation of respiratory system progenitor cells at a specified rate (ψ_s). In the initial stage of the viral diseases, the immune response is provoked to diminish the viral particle spread and relatively infected epithelial cells can be recovered when the intensity of cytopathic effect (degree of cell injury) has not induced irreversible changes. In case, HECs died after viral infection, neighbor HECs can proliferate (cell division) and replenish the infected epithelial cell at a rate of ρ. It is postulated that HECs are infected by SARS-COV2 at a rate of ξ and die naturally at a rate of μ_s.

(2) Infected epithelial cells (IECs): The term $\xi S_E V$ represents infection of HECs by the viral particles. Upon infection with the virus, HECs become the IECs type. In our developed model, the term μ_i stands for the natural mortality rate of IECs. Upon the entrance of viral particles inside the HECs, innate immune system cells eliminate the IECs by releasing different cytokines. Of note, during the initial step

Table 1: List of variables for the proposed model.

Variables	**Description**
$S_E(t)$	Density of healthy epithelial cells
$I_E(t)$	Density of infected epithelial cells
$M_1(t)$	Density of resting macrophages
$M_2(t)$	Density of activated macrophages
$C_N(t)$	Concentration of neutrophils
$C_M(t)$	Concentration of monocytes
$V(t)$	Number of virus particles
Parameters	**Description**
ψ_v	Number of SARS-COV2 released following the lysis of infected cells
η	Rate at which infected cells lyse/burst
γ_c	Rate of virus clearance by macrophages
γ_n	Rate of virus clearance by neutrophils
γ_m	Rate of virus clearance by monocyte
ψ_s	Production rate of healthy epithelial cell from stem cells
ξ	Rate of viral attachment to epithelial cell
μ_s	Natural death rate of healthy epithelial cells
μ_i	Natural death rate of infected epithelial cells
ψ_r	Macrophage birth rate
α_r	Activation rate of resting macrophage by virus
μ_r	Natural clearance rate of resting macrophages
κ	Deactivation rate of active macrophages
μ_a	Natural death rate of activated macrophages
ν_a	Virus-induced death rate of activated macrophages
ψ_n	Production rate of neutrophils induced by macrophages
μ_n	Natural death rate of neutrophils
ν_n	Virus-induced death rate of neutrophils
ψ_m	Neutrophil-induced production rate of Monocytes
μ_m	Natural death rate of monocyte
ν_m	Virus-induced death rate of monocytes

of the infection, when the number of the infected cells or intracellular dose of the virus is to some extent that innate immune response cells such as macrophages, neutrophils, and monocytes can eliminate the infected cells. By contrast, the increase of infected cells (IECs) can lead to immune system insufficiency and viral spread.

(3) Resting macrophages: In normal conditions, resting macrophages are at the constant rate of ψ_r. The number of these cells is decreased by natural death or polarization to activated macrophages (μ_r). There is permanent polarization between resting and activated macrophages depending on the inflammatory conditions. To be specific, in the presence of antigens resting macrophages are activated polarized to activated macrophages at a constant rate of α_r. Upon antigen neutralization or removal, activated macrophages are deactivated at a rate of κ.

(4) The number of activated macrophages is reduced by a natural death at a rate of μ_a. Furthermore, continuous exposure of activated macrophages to viral particles leads to cell exhaustion and atresia at the rate of ν_a.

(5) Neutrophils: The release of cytokines by activated macrophages induces neutrophils. In our model, the term ψ_n was used for this phenomenon. Neutrophils are reduced by a natural death at the rate of μ_n. The interaction and exposure of neutrophils to viral particles lead to cellular death at the rate of ν_n.

(6) Monocytes: The term $\psi_m M_2 C_M$ represents the induction and recruitment of monocytes by activated macrophages, and $\nu_m C_M V$ describes virus-induced death of monocytes at the rate of ν_m. The natural death of monocytes is shown by $\mu_m C_M$.

(7) Virus particles: The term $\eta\psi_v I_E$ represents the procedure of virus replication within epithelial cells. Here, we proposed that some fractions of viral particles are naturally at the rate of μ_v or cleared by macrophages, neutrophils, and monocytes at rates of γ_c, γ_n, and γ_m, respectively.

Some valuable features of the model

Solution's positivity

Biologically, it should be proved that if we commence with positive initial conditions, all the state variables of the COVID-19 model are positive for all t non-negative , science the number of innate immune system's cells and the virus count cannot be negative. To this end, the following theorem is crucial to be presented.

Theorem 0.1 *The region*

$$\begin{aligned} D &= \{(S_E, I_E, M_1, M_2, C_N, C_M, V) : \\ &\quad S_E > 0, I_E \geq 0, M_1 > 0, M_2 \geq 0, C_N \geq 0, C_M \geq 0, V \geq 0\}, \end{aligned}$$

is a positive invariant set for system (1).

Proof : We now show that if we commence with positive initial conditions, the solutions of system (1) stay positive for any positive t. Using the (1), we get,

$$\begin{aligned} &\frac{dS_E}{dt}\Big|_{S_E=0} = \psi_s + \rho I_E > 0, \\ &\frac{dI_E}{dt}\Big|_{I_E=0} = \xi S_E V \geq 0, \\ &\frac{dM_1}{dt}\Big|_{M_1=0} = \psi_r + \kappa M_2 > 0, \\ &\frac{dM_2}{dt}\Big|_{M_2=0} = \alpha_r M_1 V \geq 0, \\ &\frac{dC_N}{dt}\Big|_{C_N=0} = 0, \\ &\frac{dC_M}{dt}\Big|_{C_M=0} = 0, \\ &\frac{dV}{dt}|_{V=0} = \eta \psi_v I \geq 0. \end{aligned}$$

So all the right-side of above terms are non-negative on the plane (given by $S_E = 0, I_E = 0, M_1 = 0, M_2 = 0, C_N = 0, C_M = 0$, and $V = 0$, which is called bounding planes) of the non-negative region of the real space. So, if a solution commences in the inside of this region, it will stay inside it for all

future time t. This occurs because of that fact the direction of the vector field most of the times is in the direction on the bounding planes, as indicated by the above inequalities. Therefore, we deduce that if the initial conditions are positive, all the system solutions (1) stay positive for any future time $t > 0$, so the positivity of the solution for system (1) is proved.

Basic reproduction number

The COVID-19-free equilibrium (CFE) of the system (1) is gained by putting the right-hand side of the system (1), and solving the equations where $I_E = V = 0$. Then, we have

$$E_0 = (S_E^*, I_E^*, M_1^*, M_2^*, C_N^*, C_M^*, V^*) = (\frac{\psi_s}{\mu_s}, 0, \frac{\psi_r}{\mu_r}, 0, 0, 0, 0). \quad (2)$$

To proving the local stability of CFE, we apply the next-generation matrix method to the model (1). According to the [16] the F and V, defined as the new infection terms and transition terms of the infected subsystem, is formed by the differential equations for classes I_E, V, and S_E in model Eqs. 1), respectively, are presented by

$$\mathcal{F} = \begin{bmatrix} 0 & \xi\frac{\psi_s}{\mu_s} & 0 \\ \eta\psi_v & 0 & 0 \\ 0 & 0 & 0 \end{bmatrix},$$

$$\mathcal{V} = \begin{bmatrix} \mu_i + \rho & 0 & 0 \\ 0 & \mu_v & 0 \\ -\rho & \xi\frac{\psi_s}{\mu_s} & \mu_s \end{bmatrix}.$$

Therefore, the basic reproduction number ($\mathcal{R}_0$) can be obtained by calculating the spectral radius (which is defined as the largest amount of eigenvalues) of FV^{-1}. Hence

$$\mathcal{R}_0 = \frac{\xi\psi_s\eta\psi_v}{(\rho + \mu_i)\mu_s\mu_v}. \quad (3)$$

Biologically, the basic reproduction number represents the portion of each infectious and infection class (in this work, infected epithelial cells, and the

virus) in the infection procedure. Equation 3 is product of the infection rate of healthy epithelial cells by COVID-19 (ξS_E^*), number of SARS-COV2 released on lysis of infected cells($\psi - v\eta$), and the expected duration of infectiousness of SARS-COV2($\frac{1}{(\rho+\mu-i)\mu_v}$).

Local stability of CFE

For the local stability of CFE, we present the below theorem.

Theorem 0.2 *The COVID-19-free equilibrium (CFE) E_0, of the system (1), is locally stable whenever $\mathcal{R}_0 < 1$ and unstable if $\mathcal{R}_0 > 1$.*

Proof : The jacobian matrix of the system (1) around CFE (E_0) is given by

$$\mathcal{J} = \begin{bmatrix} -\mu_s & \rho & 0 & 0 & 0 & 0 & -\xi\frac{\psi_s}{\mu_s} \\ 0 & -(\mu_i+\rho) & 0 & 0 & 0 & 0 & \xi\frac{\psi_s}{\mu_s} \\ 0 & 0 & -\mu_r & \kappa & 0 & 0 & -\alpha\frac{\psi_r}{\mu_r} \\ 0 & 0 & 0 & -(\mu_a+\kappa) & 0 & 0 & \alpha\frac{\psi_r}{\mu_r} \\ 0 & 0 & 0 & 0 & -\mu_n & 0 & 0 \\ 0 & 0 & 0 & 0 & 0 & -\mu_m & 0 \\ 0 & \eta\psi_v & 0 & 0 & 0 & 0 & -\mu_v \end{bmatrix}.$$

Proving the equilibrium stability of system (1) is equivalent to proving that all eigenvalues of the Jacobin matrix are negative (here we notice that all entries of the matrix J are real). So, we prove the second part of equivalent. To do this, we transform matrix J to a higher triangular matrix $J^{'}$, and perform below row operation

$$R_7 \longrightarrow R_7 + \frac{\eta\psi_v}{\mu_i+\rho} \times R_2.$$

As a result of this operation, J is converted to a higher triangular matrix $J^{'}$ as follow

$$\mathcal{J}^{'} = \begin{bmatrix} -\mu_s & \rho & 0 & 0 & 0 & 0 & -\xi\dfrac{\psi_s}{\mu_s} \\ 0 & -(\mu_i+\rho) & 0 & 0 & 0 & 0 & \xi\dfrac{\psi_s}{\mu_s} \\ 0 & 0 & -\mu_r & \kappa & 0 & 0 & -\alpha\dfrac{\psi_r}{\mu_r} \\ 0 & 0 & 0 & -(\mu_a+\kappa) & 0 & 0 & \alpha\dfrac{\psi_r}{\mu_r} \\ 0 & 0 & 0 & 0 & -\mu_n & 0 & 0 \\ 0 & 0 & 0 & 0 & 0 & -\mu_m & 0 \\ 0 & 0 & 0 & 0 & 0 & 0 & \dfrac{\xi\psi_s}{\mu_s} \times \dfrac{\eta\psi_v}{\mu_i+\rho} - \mu_v \end{bmatrix}.$$

That allows us to identify eigenvalues directly and define stability conditions. Eigenvalues of the matrix $J^{'}$ (or roots of characteristic equation for matrix $J^{'}$) is given by the elements of the main diagonal

$$\lambda_1 = -\mu, \quad \lambda_2 = -(\mu_i+\rho), \quad \lambda_3 = -\mu_r, \quad \lambda_4 = -(\mu_a+\kappa), \quad \lambda_5 = -\mu_n,$$
$$\lambda_6 = -\mu_m, \quad \lambda_7 = \frac{\xi\psi_s}{\mu_s} \times \frac{\eta\psi_v}{\mu_i+\rho} - \mu_v.$$

All of the $\lambda_1 - \lambda_6$ is negative, so for the local stability of CFE, it is enough to the term of $\lambda_7 = \dfrac{\xi\psi_s}{\mu_s} \times \dfrac{\eta\psi_v}{\mu_i+\rho} - \mu_v$ be negative. That is mean

$$\frac{\xi\psi_s}{\mu_s} \times \frac{\eta\psi_v}{\mu_i+\rho} - \mu_v < 0,$$
$$\Longrightarrow \frac{\xi\eta\psi_v\psi_s}{\mu_v\mu_s(\mu_i+\rho)} < 1.$$

On the other hand, $\mathcal{R}_0 = \dfrac{\xi\eta\psi_v\psi_s}{\mu_v\mu_s(\mu_i+\rho)}$. Then the proof is completed.

Global stability of CFE

Theorem 0.3 *The CFE of the model system (1), given by Eq. 1, is globally asymptotically stable (GAS) in D whenever $\mathcal{R}_0 \leq 1$ and unstable otherwise.*

Proof : Suppose that

$$L = m_1 I_E + m_2 V, \tag{4}$$

be a Lyapunov function, where

$m_1 = \mu_s\mu_v + \eta\psi_v\mu_s,$
$m_2 = \xi\psi_s + \mu_s(\rho + \mu_i).$

Now, we derivative from (4) respect to the t, so we gain

$$\begin{aligned}
\dot{L} &= m_1\xi S_E V - m_1\mu_1 I_E - m_1\rho I_E + m_2\eta\psi_v I_E - m_2\mu_v V \\
&\quad - m_2(\gamma_c M_2 V + \gamma_n C_N V + \gamma_m C_M V) \\
&\leq m_1\xi S_E V - m_1\mu_1 I_E - m_1\rho I_E + m_2\eta\psi_v I_E - m_2\mu_v V \\
&= m_1\xi S_E V - m_1 I_E(\mu_1 + \rho) + m_2\eta\psi_v I_E - m_2\mu_v V \\
&= I_E[-m_1(\mu_1 + \rho) + m_2\eta\psi_v] + V[m_1\xi S_E - m_2\mu_v], \\
&(Since \;\; S_E \leq S_E^* = \frac{\psi_s}{\mu_s}) \\
&\leq I_E[-(\mu_s\mu_v + \eta\psi_v\mu_s)(\mu_i + \rho) + (\xi\psi_s + \mu_s(\rho + \mu_i))\eta\psi_v] \\
&+ V[\mu_s\mu_v\xi\frac{\psi_s}{\mu_s} + \eta\psi_v\mu_s\xi\frac{\psi_s}{\mu_s} - \xi\psi_s\mu_v - \mu_s(\rho + \mu_i)\mu_v] \\
&= I_E[\eta\xi\psi_s\psi_v - \mu_s\mu_v(\mu_i + \rho)] + V[\eta\xi\psi_s\psi_v - \mu_s\mu_v(\mu_i + \rho)] \\
&= I_E\mu_s\mu_v(\mu_i + \rho)(\mathcal{R}_0 - 1) + V\mu_s\mu_v(\mu_i + \rho)(\mathcal{R}_0 - 1) \\
&= \underbrace{(I_E + V)\mu_s\mu_v(\mu_i + \rho)}_{>0}(\mathcal{R}_0 - 1), \\
&(Since\ \mathcal{R}_0 \leq 1) \\
&\Longrightarrow \dot{L} \leq 0.
\end{aligned}$$

Since all the model parameters and variables are non-negative, it follows that $\dot{L} \leq 0$ for $\mathcal{R}_0 \leq 1$ and $\dot{L} = 0$ if and only if $I_E = V = 0$. Hence, L is a Lyapunov function on D. Furthermore, D is a compact and absorbing subset of $\mathbb{R}^8_+$, and the largest compact invariant set in $\{(S_E, I_E, M_1, M_2, C_N, C_M, V) \in D : \dot{L} = 0\}$ is the singleton E_0. Thus, by Lasalle's invariance principle ([17]), $I_E \to 0,\ V \to 0$ as $t \to \infty$. Substituting $V = I_E = 0$ into the system (1) shows that $S_E \to S_E^*, M_1 \to M_1^*, M_2 \to M_2^*, C_N \to C_N^*$, and $C_M \to C_M^*$, and as $t \to \infty$. Hence, every solution of the model system (1), with initial conditions in D, approaches the CFE, E_0, as $t \to \infty$ (that is, the CFE, E_0, is GAS in D) whenever $\mathcal{R}_0 \leq 1$.

Table 2: Values of parameters of model (1).

Parameters	**Values**	**Units**	**Sources**
$\eta.\psi_v$	19.03	$virus.cell^{-1}.day^{-1}$	[18]
γ_c	1.31	day^{-1}	[18]
γ_n	1.31	day^{-1}	Supposed
γ_m	1.31	day^{-1}	Supposed
ρ	0.02	day^{-1}	Supposed
ψ_s	4×10^{-3}	$cells.ml^{-1}.day^{-1}$	[12]
ξ	$5 \times 10^{-9} - 5.61 \times 10^{-7}$	$ml.virus^{-1}.day^{-1}$	[18]
μ_s	0.14	day^{-1}	[20]
μ_i	0.15	day^{-1}	[18]
ψ_r	0.02	day^{-1}	[19]
α_r	0.001	day^{-1}	[19]
μ_r	0.02	day^{-1}	[19]
κ	0.05-0.08	day^{-1}	[19]
μ_a	0.02	day^{-1}	[19]
ν_a	10^{-7}	$cell^{-1}$	[19]
ψ_n	4×10^{-2}	day^{-1}	Supposed
μ_n	0.01	day^{-1}	Supposed
ν_n	0.017	$cell^{-1}$	Supposed
ψ_m	$3.7 \times 10^{-}3$	day^{-1}	Supposed
μ_m	0.011	day^{-1}	Supposed
ν_m	0.024	$cell^{-1}$	Supposed
μ_v	0.07	day^{-1}	Supposed

Simulation

In this section, we analyzed the proposed model numerically. We used MATLAB software to the illustration of model dynamics especially viral load graphs. Some uncertainty parameters are found through recently published works that are cited in Table 2, and some others which are not considered on others COVID-19 works are logically assumed. In figure 3 , based on proposed model, we depict viral load process in blood by considering uncertainty parameters as follows: $\eta.\psi_v = 19.03, \gamma_c = 1.31, \gamma_n = 1.31, \gamma_m = 1.31, \psi_s = 4 \times 10^{-3}, \xi = 5 \times 10^{-9}, \mu_s = 0.14, \mu_i = 0.15, \psi_r = 0.02, \alpha_r = 0.001, \mu_r = 0.02, \kappa = 0.05, \mu_a = 0.02, \nu_a = 10^{-7}, \psi_n = 4 \times 10^{-2}, \mu_n =$

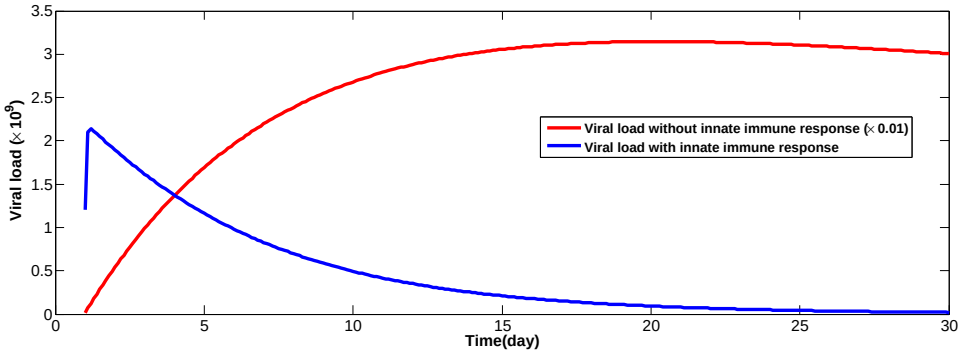

Figure 2: Viral load dynamic. The blue and red solid lines represent the viral load with and without innate immune response agains the COVID-19 virus, respectively.

$0.01, \nu_n = 0.017, \psi_m = 3.7 \times 10^{-}3, \mu_m = 0.011, \nu_m = 0.024$.

According to Figure 2 (solid blue line), the count of the virus dramatically increased in the first $2-3$ days and reached maximum levels. Upon activation of innate immune system cells, viral load is gradually decreased to the normal value in which during 30 days, near-to-normal values were achieved (see Figure 2). Next, the impact of innate immune response on systemic biodistribution of SARS-CoV-2 virus (viremia = presence of virus in the blood) was investigated. In Figures 3-6, different values associated with innate immune cells parameters were plotted. Based on data, the impact of ξ, the rate on viral attachment to epithelial cells, and viral load were assessed in Figure 3. It was suggested that there is a direct association between the ξ values and viral load levels. By increasing the ξ values, the capacity of viral load is also heightened. Commensurate with these comments, the parameter ξ has a direct effect on the replication of the SARS-CoV-2 virus. As shown in Figure 4, there is an inverse correlation between the replication of the SARS-CoV-2 virus and γ_c values (the rate of virus clearance by activated macrophages). It seems that the activation of macrophages and increased polarization of resting macrophages to activated state can help the body to clear more virions (active viral particles) directly by macrophage bioactivity or stimulation other cell types via releasing cytokines. These data support the notion that the parameter γ_c can be conceived as a prevention factor

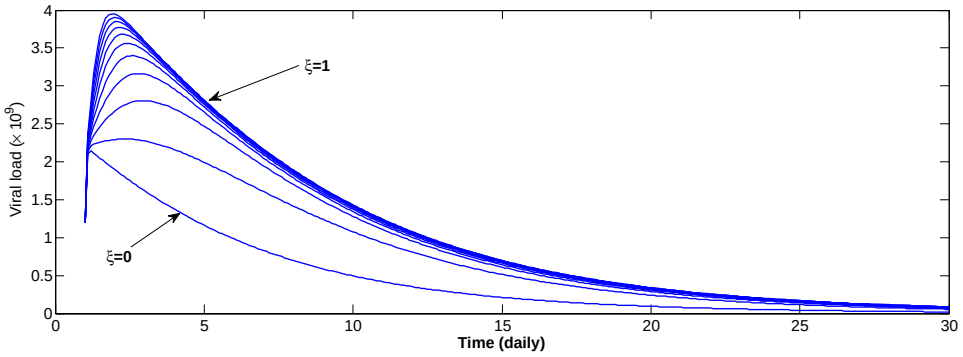

Figure 3: Viral load showing. Here, rate of viral attachment to epithelial cell (ξ) is varied between $0-1$ with $\eta.\psi_v = 19.03, \gamma_c = 1.31, \gamma_n = 1.31, \gamma_m = 1.31, \psi_s = 4 \times 10^{-3}, \mu_s = 0.14, \mu_i = 0.15, \psi_r = 0.02, \alpha_r = 0.001, \mu_r = 0.02, \kappa = 0.05, \mu_a = 0.02, \nu_a = 10^{-7}, \psi_n = 4 \times 10^{-2}, \mu_n = 0.01, \nu_n = 0.017, \psi_m = 3.7 \times 10^{-}3, \mu_m = 0.011, \nu_m = 0.024$.

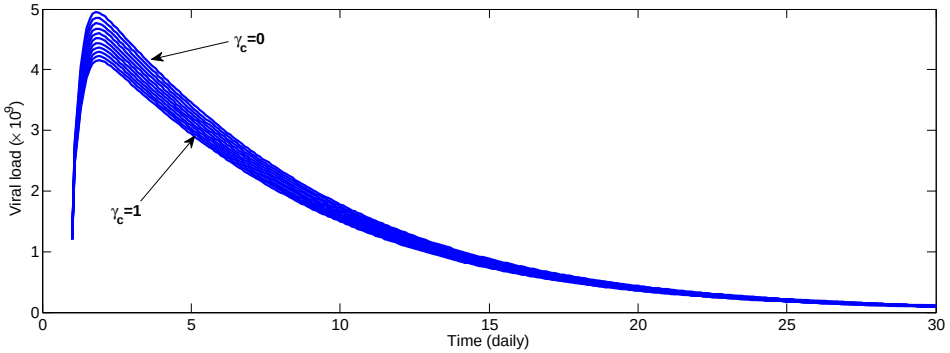

Figure 4: Viral load showing. Here, rate of virus clearance by macrophages (γ_c) is varied between $0-1$ with $\eta.\psi_v = 19.03, \xi = 5 \times 10^{-9}, \gamma_n = 1.31, \gamma_m = 1.31, \psi_s = 4 \times 10^{-3}, \mu_s = 0.14, \mu_i = 0.15, \psi_r = 0.02, \alpha_r = 0.001, \mu_r = 0.02, \kappa = 0.05, \mu_a = 0.02, \nu_a = 10^{-7}, \psi_n = 4 \times 10^{-2}, \mu_n = 0.01, \nu_n = 0.017, \psi_m = 3.7 \times 10^{-}3, \mu_m = 0.011, \nu_m = 0.024$.

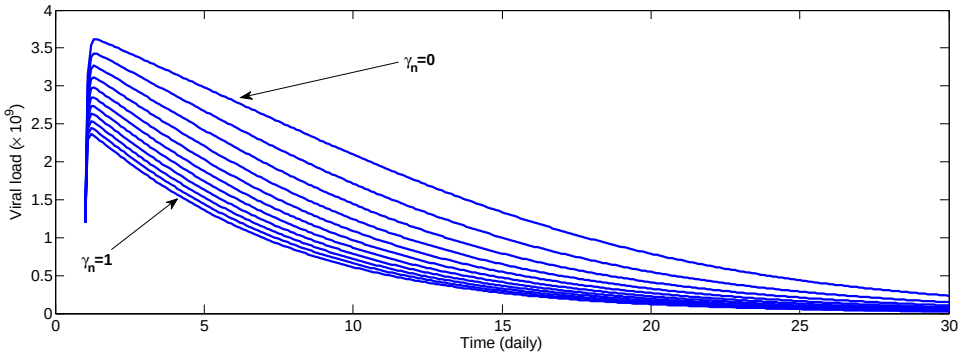

Figure 5: Viral load showing. Here, rate of virus clearance by neutrophils (γ_n) is varied between $0-1$ with $\eta.\psi_v = 19.03, \gamma_c = 1.31, \gamma_m = 1.31, \psi_s = 4 \times 10^{-3}, \xi = 5 \times 10^{-9}, \mu_s = 0.14, \mu_i = 0.15, \psi_r = 0.02, \alpha_r = 0.001, \mu_r = 0.02, \kappa = 0.05, \mu_a = 0.02, \nu_a = 10^{-7}, \psi_n = 4 \times 10^{-2}, \mu_n = 0.01, \nu_n = 0.017, \psi_m = 3.7 \times 10^{-}3, \mu_m = 0.011, \nu_m = 0.024$.

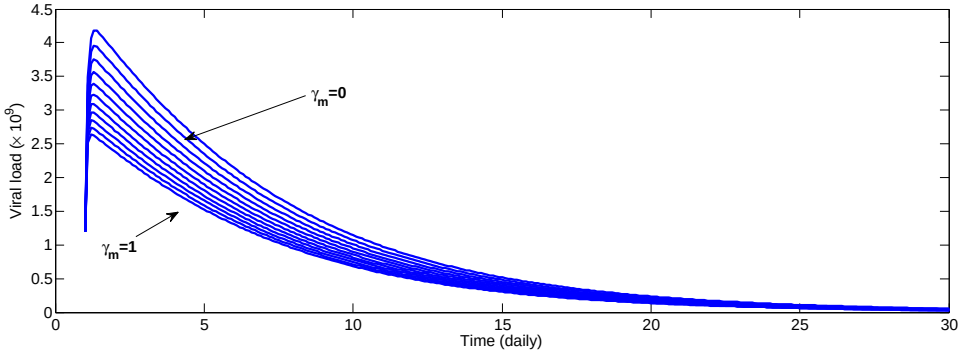

Figure 6: Viral load showing. Here, rate of virus clearance by monocyte (γ_m) is varied between $0-1$ with $\eta.\psi_v = 19.03, \gamma_c = 1.31, \gamma_n = 1.31, \psi_s = 4 \times 10^{-3}, \xi = 5 \times 10^{-9}, \mu_s = 0.14, \mu_i = 0.15, \psi_r = 0.02, \alpha_r = 0.001, \mu_r = 0.02, \kappa = 0.05, \mu_a = 0.02, \nu_a = 10^{-7}, \psi_n = 4 \times 10^{-2}, \mu_n = 0.01, \nu_n = 0.017, \psi_m = 3.7 \times 10^{-}3, \mu_m = 0.011, \nu_m = 0.024$.

following COVID-19 infection. It can be postulated that the increase of activated macrophages in target tissues and circulating monocytes can be proposed as a defensive mechanism in response to viral infection. Therefore, any modalities that contribute to in situ macrophage density via enhanced polarization and monocyte recruitment can be proposed as a therapeutic strategy. Fortunately, this approach is possible in a clinical setting after the conduction of laboratory experiments. In Figures 5 and 6, it was notified that reducing viral load can result in the elevation of blood neutrophils and monocytes, respectively. This effect is associated with the reduced recruitment of these cells from the blood into the affected area. The reduction of neutrophils and monocytes would be related to severe viral infection and higher epithelial cell infectivity that need urgent recruitment of neutrophils and monocytes. Also, based on Figure 4-6, it was graphically proven that the impact of monocytes count is higher than neutrophil in order to viral clearance, and activated macrophages have the strongest influence.

Conclusion

We mathematically modeled the interaction between SARS-CoV-2 and innate immune cells as an in-host model. In this model, we considered the most effective innate immune cells against SARS-CoV-2 like macrophages, neutrophils, and monocyte. In the modeling procedure, we discussed the transmission of the virus to the blood and how innate immune cells act against this virus. Also, based on mathematical approaches, we analyzed the stability of the proposed model. Here, the question is this: how this research can be beneficial, and how other researchers can take advantage of the present study. To answer this question, we recall the result of the simulation section. Because we proved the impact of the vital parameters in the model versus the virus, related researchers in vaccine development will be able to use these results in their study. In future work, we can investigate this study on different classes of people, and explore the impact of the innate immune response of different people against the virus.

Data availability

No datasets were generated or analyzed during the current study.

References

[1] McNeill, W. H. Plagues and peoples. 183–240 (New York: Bantam Doubleday Dell Publishing Group, 1976).

[2] Institute of Medicine (US) Forum on Microbial Threats. Microbial Evolution and Co-Adaptation: A Tribute to the Life and Scientific Legacies of Joshua Lederberg: Workshop Summary. 195–208 (Washington (DC): National Academies Press (US), 2009).

[3] World Health Organization. COVID-19 weekly epidemiological update (WHO, 13 July 2021)
https://www.who.int/publications/m/item/weekly-epidemiological-update-on-covid-19—13-july-2021.

[4] Santos, D. & Gouvea, W. Impact of virus genetic variability and host immunity for the success of COVID-19 vaccines. *Biomed. Pharmacother.*111282; 10.1016/j.biopha.2021.111272 (2021).

[5] Xingyu, L. *et al.* Mathematical model of the feedback between global supply chain disruption and COVID-19 dynamics. *Sci. Rep.* **11**. 15450; 10.1038/s41598-021-94619-1 (2021).

[6] Agapiou, A. *et al.* Modeling the first wave of Covid-19 pandemic in the Republic of Cyprus. *Sci. Rep.* **11**. 7342; 10.1038/s41598-021-86606-3 (2021).

[7] Ndaïrou, F. *et al.* Mathematical modeling of COVID-19 transmission dynamics with a case study of Wuhan. *Chaos Solitons Fractals.* **135**. 109846; 10.1016/jchaos109846 (2020).

[8] Giordano, G. *et al.* Modelling the COVID-19 epidemic and implementation of population-wide interventions in Italy. *Nat. Med.* **26** 855–860 (2020).

[9] Ivorra, B., Ferrández, M. R., Vela-Pérez, M., Ramos.& Angel, M. Mathematical modeling of the spread of the coronavirus disease 2019 (COVID-19) taking into account the undetected infections. The case of China. *Commun Nonlinear Sci Numer Simul.* **88**. 105303; 10.1016/jcnsns.105303 (2020).

[10] Peng, L., Yang, W., Zhang, D., Zhuge, C. & Hong, L. Epidemic analysis of COVID-19 in China by dynamical modeling. preprinted at https://arxiv.org/abs/2002.06563 (2020).

[11] Musa, S. *et al.* Mathematical modeling of COVID-19 epidemic with effect of awareness programs. *Infect. Dis. Model.* **6**. 448–460 (2021).

[12] Hernandez-Vargas, E. A. & Velasco-Hernandez, J. X. In-host mathematical modelling of COVID-19 in humans. *Annu Rev Control.* **50**. 448–456 (2020).

[13] Li, C. T., Xu, J. H., Liu, J. W., & Zhou, Y. C. The within-host viral kinetics of SARS-CoV-2. *Math Biosci Eng.* **17**. 2853–2861 (2020).

[14] Du, S. Q. & Yuan, W. Mathematical modeling of interaction between innate and adaptive immune responses in COVID-19 and implications for viral pathogenesis. *J. Med. Virol* **92**. 1615–1628 (2020).

[15] Schultze, J. L. & Aschenbrenner, A. C. COVID-19 and the human innate immune system. *Cell.* **184** 1671-1692 (2021).

[16] Diekmann, O., Heesterbeek, J. A. & Metz, J. A. On the definition and the computation of the basic reproduction ratio $\mathcal{R}_0$ in models for infectious diseases in heterogeneous populations. *J Math Biol.* **28**. 365–382 (1990).

[17] Hale, J. K. Dynamical systems and stability. *J. Math. Anal. Appl.* **26**. 39–59 (1969).

[18] Dogra, P. *et al.* Innate immunity plays a key role in controlling viral load in COVID-19: mechanistic insights from a whole-body infection dynamics model. preprinted at https://www.ncbi.nlm.nih.gov/pmc/articles/PMC7654909/ (2020).

[19] Eftimie, Ra. & Hamam, H. Modelling and investigation of the CD4+ T cells–Macrophages paradox in melanoma immunotherapies. *J. Theor. Biol.* **420**. 82–104 (2017).

[20] Sasmal, S. K., Dong, Y. & Takeuchi, Y. Mathematical modeling on T-cell mediated adaptive immunity in primary dengue infections. *J. Theor. Biol.* **429**. 229–240 (2017).

Acknowledgements

We thank Prof. Abba B. Gumel for many helpful and constructive discussions.

Author contributions

Mehdi Lotfi developed the modeling section and wrote code for the simulations. Azizeh Jabbari and Hossein Kheiri developed mathematics analysis sections. Also, Reza Rahbarghazi wrote the medical and biological interpretation of modeling and simulation sections. All authors reviewed the manuscript.

Competing interests

The authors declare no competing interests.